Biodegradable and Porous Poly(lactic-*co*-glycolic acid) Microbeads for *In vitro* Evaluation of Negatively Charged Fluorescent Bacteria

Tian Qiao[1]
Soohyun Kim[1]
Wonmok Lee[2]
Hyunjung Lee*,[1]

[1] School of Advanced Materials Engineering, Kookmin Univ., Jeongneung gil 77, Seongbuk-gu, Seoul 02707, Korea

[2] Department of Chemistry, Sejong Univ., Neungdong-ro 209, Gwangjin-gu, Seoul 143747, Korea

Abstract: In this study, porous microbeads synthesized by water-oil-water [water/oil/water ($W_1/O/W_2$)] double-emulsion solvent evaporation method exhibited immense potential as biocarriers for the attachment of bacteria. Poly(lactic-*co*-glycolic acid) (PLGA) was selected as a biodegradable, biocompatible material for fabricating porous microbeads. Ammonium bicarbonate and polyvinyl alcohol concentrations played a significant role in the modification of the microbead size. The microbead surface structure was modified by partial hydrolysis using sodium hydroxide to generate open pores on the surface and a more hydrophilic surface than PLGA itself. To examine the inner morphology of the microbeads, confocal laser scanning microscopy was employed in combination with rhodamine B during the fabrication of porous microbeads. Finally, the attachment of fluorescent bacteria to these porous microbeads was analyzed in terms of affinity between bacteria and porous PLGA microbeads. The affinity of microbeads to negatively charged bacteria was observed as a function of the charges of the PLGA microbead surfaces, indicating that surface-modified PLGA porous microbeads decorated with positively charged chitosan exhibit an enhanced affinity to negatively charged bacteria.
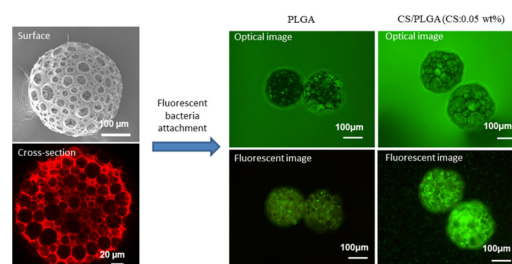
Keywords: PLGA, porous microbeads, surface modification, bacterial attachment.

1. Introduction

Microbeads demonstrate widespread applications in sensors for the determination of trace amounts of toxins, monitoring of environmental pollutants, and analysis of food and biomedicine because of their rapid response, cost-effectiveness, and high sensitivity.[1-5] In particular, the use of microbead sensors for the distinction between several nitrogen-containing compounds in soil has attracted considerable attention in terms of monitoring contaminated soil, maintaining explosive materials in military regions, or investigating spoiled foods.[6-8]

To enhance the sensitivity or accuracy of microbead-based sensors, several issues have been currently raised with respect to microbeads. First, the selection of sensor material is crucial in this study. Meanwhile, hydrogels have also been widely used in bioengineering applications; however, hydrogels exhibit intrinsic drawbacks, such as low mechanical strength and durability.[9,10]

In particular, a typical hydrogel, *i.e.*, alginate hydrogel microbeads, physically cross-linked with ions, exhibits low durability and can be easily broken by other ionic species. On the other hand, PLGA has been considered a biodegradable scaffold with higher durability in soil. Besides, it undergoes hydrolysis, leading to decomposition into small fragments such as original monomers, lactic acid and glycolic acid. Under normal physiological conditions, lactic acid and glycolic acid are the typical by-products obtained from various metabolic pathways in the body and are environmentally friendly to the surrounding soil conditions.

Second, the surface topography and microbead structure are crucial for high-performance sensors. Biodegradable and biocompatible porous microbeads have been universally used in bioengineering fields, such as cell culture, drug delivery, tissue engineering, and bacterial attachment.[11-15] Necrosis of cell and aerobic bacteria often occurs because of the insufficient supply of nutrients or oxygen and the accumulation of metabolic wastes.[16-18] Microbeads with an open porous structure can effectively overcome this drawback because of their large surface area related to the presence of inner pores as well as open surface pores, thereby affording suitable scaffolds or carriers for cell culture and bacterial attachment.

Third, the high affinity of cells or bacteria to microbeads is crucial for the improved behavior of microbead-based biosensors. Improving the cell affinity to microbead-based sensors has attracted considerable attention. Qin *et al.* have reported that biodegradable and biocompatible PLGA microbeads can be used as carriers for cell culture.[19] However, the inherent hydro-

phobic surface of PLGA material limits cell attachment. To overcome this drawback, partial hydrolysis of the surface has to be performed to modify the PLGA microbead surface and render it hydrophilic via the generation of hydroxyl and carboxyl groups.

In this study, porous microbeads that were used as carriers for loading bacteria in biosensors were prepared. First, the water/oil/water ($W_1/O/W_2$) method was employed to fabricate porous structure microbeads. Ammonium bicarbonate (NH_4HCO_3), which is an effervescent salt, was homogeneously mixed in the primary aqueous phase to generate carbon dioxide (CO_2) and ammonia (NH_3) gas bubbles after solvent evaporation. In addition, sodium hydroxide (NaOH) was used to partially hydrolyze the PLGA microbead surface to generate open pores on the surface and render the PLGA microbead surface hydrophilic. To enhance the attachment of negatively charged bacteria, the surface charge of PLGA microbeads should be controlled. Therefore, the surface charge of PLGA microbeads was modified using chitosan having positive surface charges. Finally, these modified microbeads were used as a biosensor by attachment with fluorescent bacteria.

As fluorescent bacteria, Escherichia coli BL21(DE3) carrying a pBbE7K-gfp+ plasmid that expresses an improved green florescent protein (GFP) under the control of the isopropyl β-D-1-thiogalactopyranoside (IPTG)-inducible T7 promoter, which was constructed by transforming the *E. coli* strain BL21(DE3) with the GFP plasmid, was used.[20] pBbE7K-gfp+ is a plasmid containing the gene encoding gfp+. The plasmid was constructed by replacing the rfp region of BioBrick plasmid pBbE7K-RFP with this gfp+. GFP, which emits a green fluorescence at 535 nm, can be expressed and produced after the induction of IPTG during culture. Figures S1 and S2 in the Supplementary information show the structure of the plasmid of this gene-modified E. coli and the induction mechanism, respectively.

2. Experimental

2.1. Materials

PLGA (lactide:glycolide=75:25, MW=66,000-107,000) and NH_4HCO_3 were purchased from Sigma-Aldrich, Inc., USA. Dichloromethane (DCM) and NaOH were obtained from Daejung Chemicals & Metals Co., Ltd. Polyvinyl alcohol (PVA) was purchased from Junsei Chemical Co., Ltd., Japan. Rhodamine B was purchased from Sigma-Aldrich, Inc., USA. All chemicals were analytical grade and were used as received without further purification.

2.2. Synthesis of porous microbeads

First, 2 mL of deionized (DI) water containing NH_4HCO_3 were added to 7 mL of DCM containing 240 mg PLGA. The first water/oil (W_1/O) emulsion was prepared using a homogenizer at 12000 rpm for 3 min. This primary emulsion was immediately transferred into a beaker containing 150 mL of a 0.1 wt% PVA solution and then re-emulsified using an overhead propeller for >4 h at 200 rpm.[21] After the complete evaporation of the solvent by stirring with an overhead propeller, the microbeads

were separated using a standard sieve with a mesh diameter of 75 μm and washed 3 times with DI water. Next, a 0.2 M NaOH solution (pH 13) was used to hydrolyze the microbeads for 5-30 min. After hydrolysis using the NaOH solution, microbeads were washed again three times using DI water to remove the remaining NaOH solution. For fabricating porous microbeads loaded with rhodamine B, 4 mM of rhodamine B was mixed into the first aqueous phase before the first w/o emulsion.

2.3. Characterization

Scanning electron microscopy (SEM; JEOL LTD., Japan) images were recorded to observe the morphology of the microbeads under different synthesis parameters. Image J (image analysis) software using SEM images was used to analyze the diameters of the microbeads and pores. The average diameters of the microbeads and pores were averaged by counting 50 microbeads and 100 pores, respectively. The zeta potentials of PLGA microbeads and chitosan-coated PLGA microbeads (CS/PLGA) were calculated using a zeta potential/particle sizer system (NICOMP, 380 ZLS). The average value was obtained by measuring 3 sets in each group. Confocal laser scanning microscopy (Leica, TCS SP5) images were recorded at an excitation wavelength of 553 nm by loading rhodamine B dyes to observe the cross-section image of porous microbeads. The attachment behavior of fluorescent bacteria was observed using a fluorescence microscope (Nikon, Eclipse Ti, Japan). The optical density (OD) values of the bacterial solution were recorded using a UV/Vis spectrometer (Perkin Elmer) at 600 nm. The porosity of porous microbeads was measured by mercury intrusion porosimetry (AutoPore IV 9520).

2.4. Chitosan-coated PLGA microbeads

Chitosan solutions at concentrations of 0.05, 0.1, and 0.2 wt% were prepared by the addition of chitosan powders into DI water with vigorous stirring overnight. Filtration was performed to remove the impurities in the chitosan solution using a sieve with a mesh diameter of 75 μm. Four groups of 0.1 g PLGA microbeads were immersed into various concentrations of chitosan solutions in a 5 mL glass vial for 6 h. Then, CS/PLGA microbeads were washed three times using DI water. CS/PLGA microbeads were used to calculate the zeta potential and bacterial attachment behavior.

2.5. Bacteria culture

E. coli BL21 (DE3) carrying pBbE7K-gfp+ plasmid colonies were transferred into a 50 mL centrifuge tube, and 20 mL of the Luria-Bertani (LB) broth medium and 20 μL of kanamycin were added. After 8 h, 20 μL of IPTG as the autoinducer was added to the bacterial culture solution. After the cultivation was incubated for 18 h at 200 rpm, the bacterial solution concentration was measured using a UV-vis spectrometer at 600 nm, and the OD value of the bacterial solution was set as 1.0 by dilution with the LB broth medium at 600 nm.

Porous PLGA and CS/PLGA microbeads were immersed into

the bacterial solution, the OD value of which was 1.0. After 12 h, the microbeads were washed three times using phosphate-buffered saline, and the bacteria attached to the microbeads were observed by fluorescence microscopy.

3. Results and discussion

3.1. Preparation of porous microbeads

Figure 1 illustrates the schematic of the fabrication of porous microbeads. Porous PLGA microbeads were fabricated by the $W_1/O/W_2$ double emulsion method with the addition of NH_4HCO_3 in the inner W_1 droplets for generating gas bubbles. The oil phase (O) was DCM containing PLGA. The W_1 droplets dispersed in the oil phase finally changed into pores. The NH_4HCO_3 dissolved in the W_1 droplets generated gas bubbles (NH_3 and CO_2), which played a significant role in maintaining a stable emulsion because an additional surfactant was not used in the primary W_1/O emulsion.[21,22] In addition, these gas bubbles changed into secondary small pores, which could be considered as the pathways among the large pores. In total, this experiment lasted for at least 4 h because of the sufficient evaporation of organic solvents. During evaporation in the second emulsification step, the oil phase became viscous and elastic with the gradual removal of organic solvent, which finally solidified.

Table 1 summarizes the porosities of the fabricated PLGA microbeads. By modifying the concentration of NH_4HCO_3, the 1st emulsification rpm and the water oil ratio, the various microbeads were fabricated. And Figure S3 shows the morphology of these four groups of microbeads. All of the groups show the very high porosities around 90%, which could promote the attachment of fluorescent bacteria.

3.2. Effect of NH_4HCO_3 concentration

Figure 2 shows the SEM images of PLGA microbeads prepared by the incorporation of different amounts of NH_4HCO_3 in the W_1 aqueous phase. The average diameters of microbeads prepared using 5 and 10 wt% NH_4HCO_3 were 187±50 μm and 427±80 μm, respectively. The generation of gas bubbles within the W_1 phase droplets surrounded by the viscous and elastic PLGA phase enabled the W_1 phase droplets to contribute to the increase of the total solution volume. Meanwhile, the small gas bubbles that changed and escaped from the aqueous droplets into the oil phase also led to the increased volume of the PLGA skeletal backbone.[19] High NH_4HCO_3 concentrations generated more gas bubbles, thereby clearly increasing the microbead volume. Thus, the NH_4HCO_3 incorporated within the primary emulsion droplets as a dispersed aqueous phase clearly contributes to the increased size of PLGA microbeads.[21]

3.3. Effect of NaOH treatment time

These synthesized microbeads did not exhibit open pores on their surface (Figure 2), which could make the access of biomaterials difficult in some bioapplications. To overcome this issue, partial hydrolysis was performed to generate open pores on the PLGA microbead surface. Because PLGA comprises several
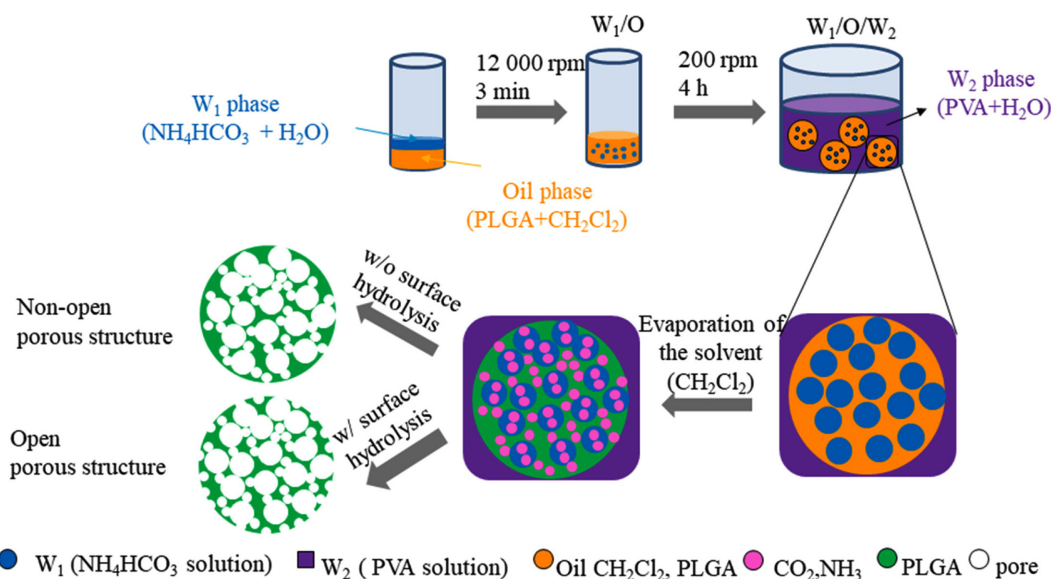

Figure 1. Schematic of the fabrication of porous PLGA.

Table 1. Porosity of PLGA microbeads under different experimental conditions

No.	Material	NH_4HCO_3 (wt%)	1st emulsification (rpm)	Water:oil (vol:vol)	PVA (wt%)	Porosity (%)
Group 1	PLGA (75:25)	5	6000	6:21	1	89.20
Group 2	PLGA (75:25)	5	12000	6:21	1	88.99
Group 3	PLGA (75:25)	5	6000	8:21	1	89.19
Group 4	PLGA (75:25)	2.5	6000	6:21	1	92.91
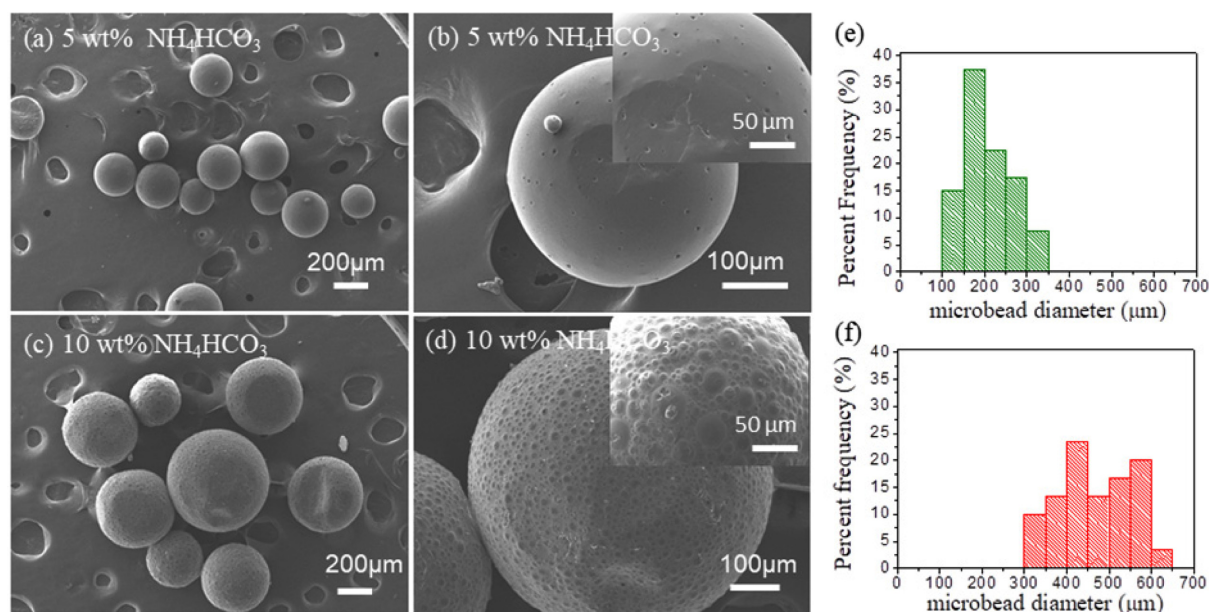
Figure 2. Effect of NH_4HCO_3 concentration on diameter of microbeads. (a-d) SEM images of the porous PLGA microbeads prepared from a primary emulsion including 5 wt% (a, b) and 10 wt% (c, d) NH_4HCO_3 in the W_1 phase, respectively. (e, f) Diameter distribution of porous PLGA microbeads with 5 wt% and 10 wt% of NH_4HCO_3. (Fabrication condition: oil phase: 2.5 wt% PLGA in 3.5 mL CH_2Cl_2, W_2 phase: 0.1 wt% PVA.) Insets: High-magnification SEM images of the corresponding microbeads in (b) and (d).
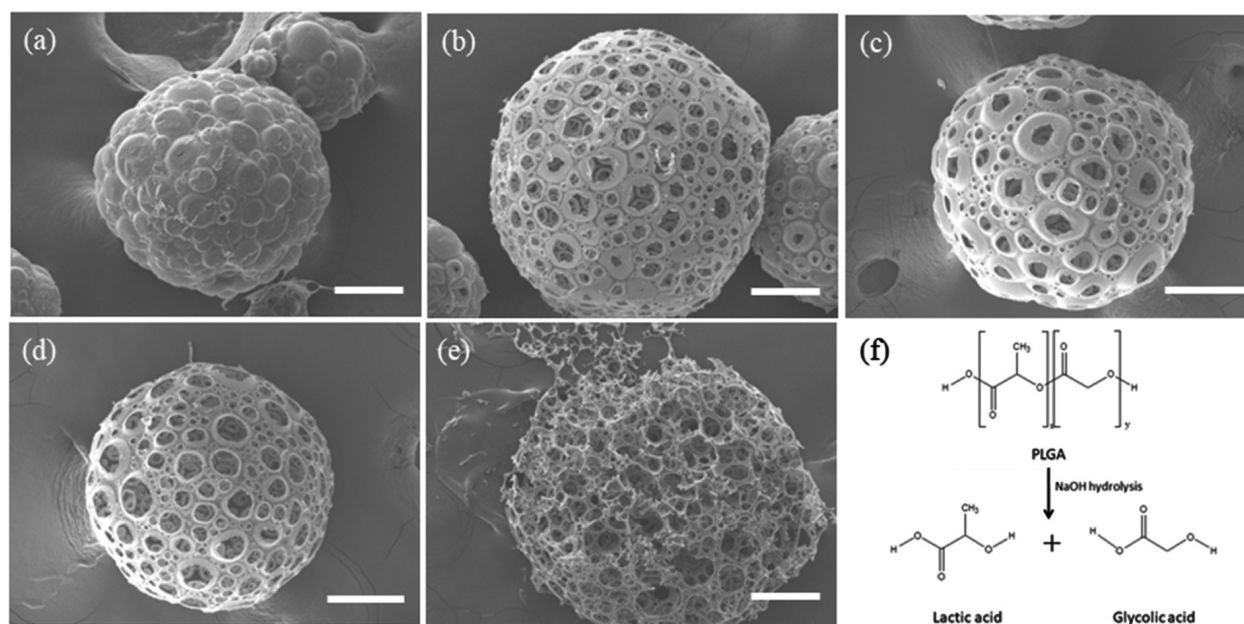
Figure 3. NaOH solution treatment to generate an open porous structure as a function of treatment time. (a) Original microbeads without NaOH treatment. (b-e) Open porous microbeads with 0.2 M NaOH treatment for 5, 20, 25, and 30 min, respectively. All scale bars indicate 100 μm. (Fabrication condition: W_1 phase: 1 mL of a 5 wt% NH_4HCO_3 solution, oil phase: 2.5 wt% PLGA in 3.5 mL CH_2Cl_2, W_2 phase: 0.1 wt% PVA.)
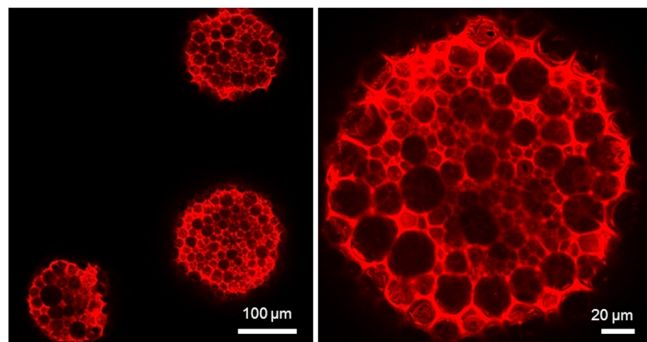
ester bonds, an alkaline NaOH solution leads to the accelerated decomposition of the ester bonds, ultimately contributing to the open porous surface structure.[15,23]

Figure 3 shows the morphologies of the microbeads as a function of the NaOH treatment time from (a) to (e), and the hydrolysis mechanism is shown in (f). Figure 3(a) shows the non-open porous structure without NaOH treatment, and Figures (b)-(e) show different morphologies with the open porous structure as a function of the NaOH treatment time. The longer the treatment time, the higher the degree of open pores is on the surface. In (e), an extremely long treatment time destroyed the porous microbead skeleton. Besides, hydrolysis treatment led to the modification of the surface property of PLGA microbeads, *i.e.*, it rendered the PLGA microbead surfaces hydrophilic *via* the creation of active functional groups (*e.g.*, carboxyl and hydroxyl),[24] and provided a relatively bioactive, suitable hydrophilic surface for the attachment of fluorescent bacteria.

3.4. Confirmation of the inner porous structure of porous PLGA microbeads by confocal laser scanning microscopy

Conventionally, physical cutting to obtain a cross-section of the microbeads cannot be performed for PLGA microbeads because it is difficult to obtain a cross-section without destroying the inner microbead structure because PLGA is soft. To observe the morphology of the microbead cross-section, confocal laser scanning microscopy was employed in addition to mixing rhodamine B in the W_1 phase during the $W_1/O/W_2$ double emulsion method.

The porous microbead skeleton was labeled with fluorescent rhodamine B (Figure 4). After excitation with incident light at 553 nm, only the region labeled with rhodamine B exhibited strong fluorescence. Dark circles in Figure 4 represent the existence of pores.

Figure 4. Confocal laser scanning microscopy images of rhodamine B-loaded PLGA microbeads. (Fabrication condition: W_1 phase: 1 mL of a 5 wt% NH_4HCO_3 solution, oil phase: 2.5 wt% PLGA in 3.5 mL CH_2Cl_2, W_2 phase: 0.1 wt% PVA, NaOH solution: 0.2 M, treatment time: 25 min, Rhodamine B dye concentration: 4 mM.)

3.5. Effect of PVA concentration

The sizes of the microbeads fabricated using 0.1 and 1 wt% PVA were 932±290 µm and 308±61 µm, respectively (Figure 5). With the decrease in the PVA concentration in the W_2 phase, the microsphere size clearly increased. PVA, serving as a surfactant, was incorporated into the W_2 phase to stabilize W_1/O and W_2 to prevent the coalescence of the oil droplets with the surrounding by the PVA solution. In contrast, PVA is a high-molecular-weight polymer, and its presence in the W_2 phase can increase the viscosity of the double emulsion, leading to an increased difficulty in breaking up the emulsion into smaller droplets.[25,26] High PVA concentration led to the production of microbeads with a small diameter, but a considerable difference on the pore sizes within their standard deviations was not observed (Figure 5).
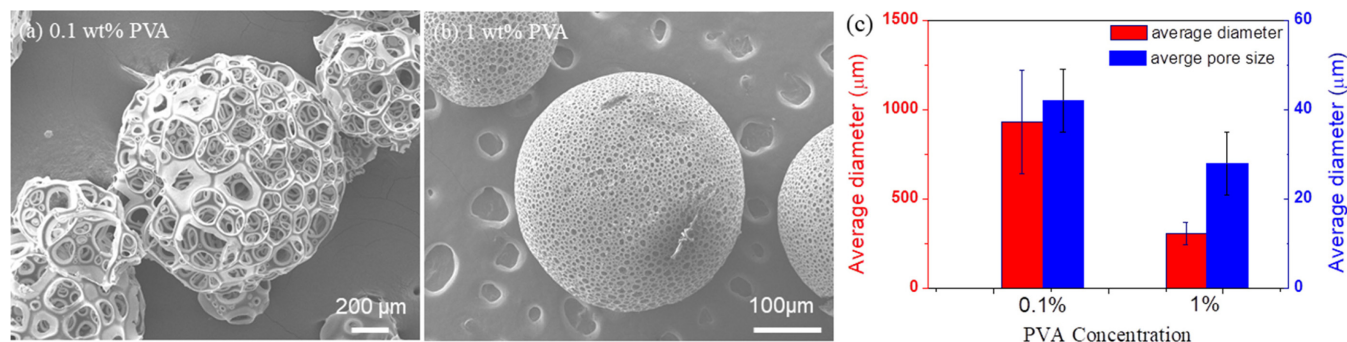
Figure 5. Microbead diameter and pore size as functions of the PVA concentration. (a-b) SEM images of PLGA microbeads prepared using different PVA concentrations in the second aqueous phase (W_2), (a) 0.1% wt%, (b) 1 wt%. (Fabrication condition: W_1 phase: 1 mL of a 5 wt% NH_4HCO_3 solution, oil phase: 2.5 wt% PLGA in 3.5 mL CH_2Cl_2, NaOH solution: 0.2 M, treatment time: 25 min.) (c) The summary of microbead diameter and pore size in case of 0.1% wt% and 1 wt% PVA in second aqueous phase.
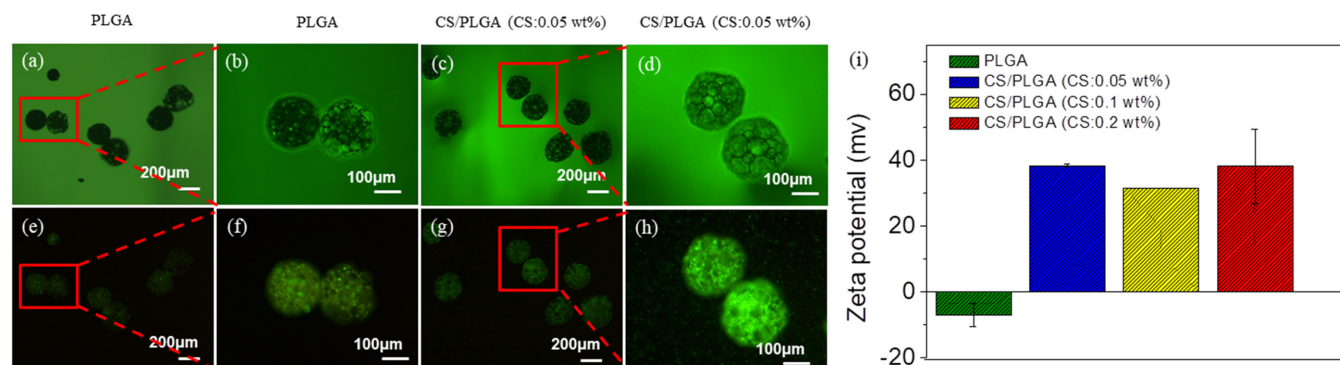
Figure 6. Bacteria attachment ability and Zeta potentials for PLGA and CS/PLGA microbeads (a-h) Comparison between PLGA and CS/PLGA as biocarriers with fluorescent *E. coli*. (Images a, b, c, and d are typical optical images with the green light as incident light. Images e, f, g, and h are fluorescence images with the blue light as incident light for the same microbeads in (a), (b), (c), and (d). Images b, d, f, and h are high-magnification images of a, c, e, and g). (Fabrication condition: W_1 phase: 1 mL of a 5 wt% NH_4HCO_3 solution, oil phase: 2.5 wt% PLGA in 3.5 mL CH_2Cl_2, W_2 phase: 200 mL of 0.1 wt% PVA, NaOH solution: 0.2 M, treatment time: 25 min.) (i) Zeta potentials of pristine PLGA and CS/PLGA.

3.6. Attachment of fluorescent bacteria

PLGA microbeads exhibited a negatively charged surface, and their surface charge was modified with a positively charged surface by coating with chitosan, which is a typical material to imparting a strongly positively charged surface (Figure 6). Figures 6(a)-(h) show the optical microscopy images of PLGA and CS/PLGA microbeads attached with fluorescent bacteria. CS/PLGA microbeads exhibited brighter green fluorescence with a higher intensity than that of the PLGA microbeads, indicating that positively charged CS/PLGA microbeads exhibit a higher affinity to negatively charged bacteria caused by electrostatic force, and a greater number of fluorescent bacteria were attached to CS/PLGA microbeads.[27-29] Due to the electrostatic interaction of anionic PLGA polymers and cationic chitosan molecules, the chitosan was successfully coated on the surface of PLGA microbead.[30,31] As shown in Figure 6(i), after coating with chitosan, the zeta potential of PLGA was changed from -7.0±3.6 mv to 38.5±0.4 (0.05 w% CS), 31.6±0.1(0.1 w% CS) and 38.2±11.2 (0.2 w% CS) mv, respectively. Considering the standard deviation, there is no significant effect on chitosan concentration. The 0.05 w% CS showed a saturated zeta potential of CS/PLGA microbeads.

4. Conclusions

In this study, microbeads with an open porous structure were synthesized by a double emulsion method combined with surface modification techniques, such as partial hydrolysis and additional coating with positively charged chitosan. The PLGA microbead porous structure was confirmed by SEM images of the porous surface structure and confocal laser scanning microscopy images of the inner porous structure. In addition, a hydrolysis time of 25 min was optimal for generating open porous structures, and the porosity of these porous PLGA microbeads was ~90%. With the increase in the NH_4HCO_3 concentration from 5 to 10 wt%, the mean diameter of PLGA microbeads increased from 187±50 μm to 427±80 μm. With the decrease in the PVA concentration from 1.0 to 0.1 wt%, the average diameter of microbeads increased from 308±61 μm to 932±290 μm. Coating with positively charged chitosan on PLGA microbeads proved to be an alternative strategy for increasing cell affinity. These CS/PLGA microbeads demonstrate potential as carriers of biomaterials, such as fluorescent bacteria. In our future research, these porous microbeads are expected to serve as highly efficient biosensors.

Supporting Information: Information is available regarding the structure of the plasmid of E. coli BL21 (DE3) pBbE7k-egfp+, induction mechanism of IPTG for GFP expression and morphology of porous PLGA microbeads summarized in Table 1. The materials are available *via* the Internet at http://www.springer.com/13233.

References

(1) Z. Yan, C. Tian, X. Qu, W. Shen, and B. Ye, *Colloid Surface B*, **154**, 142 (2017).

(2) C. Sun, R. Sun, Y. Chen, Y. Tong, J. Zhu, H. Bai, S. Zhang, H. Zheng, and H. Ye, *Sens. Actuators B*, **255**, 775 (2018).

(3) S. Lee, Y.-L. Lee, B. Kim, K. Kwon, J. Park, K. Han, H. Lee, and W. Lee, *Sens. Actuators B*, **231**, 256 (2016).

(4) S. Kim, S. G. Han, Y. G. Koh, H. Lee, and W. Lee, *Sensors (Basel)*, **18**, 1357 (2018).

(5) Z. Liao, Y. Zhang, L. Su, J. Chang, and H. Wang, *J. Nanopart. Res.*, **19**, 60 (2017).

(6) Y. Kabessa, O. Eyal, O. Bar-On, V. Korouma, S. Yagur-Kroll, S. Belkin, and A. J. Agranat, *Biosens. Bioelectron.*, **79**, 784 (2016).

(7) H. Turhan, E. Tukenmez, B. Karagoz, and N. Bicak, *Talanta*, **179**, 107 (2018).

(8) W. Lu, S.A. Asher, Z. Meng, Z. Yan, M. Xue, L. Qiu, and D. Yi, *J. Hazard. Mater.*, **316**, 87 (2016).

(9) S. K. Sahoo, A. K. Panda, and V. Labhasetwar, *Biomacromolecules*, **6**, 1132 (2005).

(10) Y. Senuma, S. Franceschin, J. Hilborn, P. Tissieres, I. Bisson, and P. Frey, *Biomaterials*, **21**, 1135 (2000).

(11) S. L. Yao, Y. D. Yang, X. M. Wang, and L. N. Wang, *Macromol. Res.*, **25**, 528 (2017).

(12) J. E. Song, N. Tripathy, J. H. Shin, D. H. Lee, J. G. Cha, C. H. Park, D. S. Suh, and G. Khang, *Macromol. Res.*, **25**, 994 (2017).

(13) S.-W. Choi, Y. Zhang, Y.-C. Yeh, A. Lake Wooten, and Y. Xia, *J. Mater. Chem.*, **22**, 11442 (2012).

(14) H. K. Kim, H. J. Chung, and T. G. Park, *J. Control. Release*, **112**, 167 (2006).

(15) X. Shi, J. Jiang, L. Sun, and Z. Gan, *Colloid Surface B*, **85**, 73 (2011).

(16) S. M. Lim, H. J. Lee, S. H. Oh, J. M. Kim, and J. H. Lee, *J. Biomed. Mater. Res. B*, **90**, 521 (2009).

(17) V. I. Sikavitsas, G. N. Bancroft, and A. G. Mikos, *J. Biomed. Mater. Res. A*, **62**, 136 (2002).

(18) J. Yang, M. Yamato, C. Kohno, A. Nishimoto, H. Sekine, F. Fukai, and T. Okano, *Biomaterials*, **26**, 6415 (2005).

(19) J. Ma, Y. S. Hui, M. Zhang, Y. Yu, W. Wen, and J. Qin, *Small*, **9**, 497 (2013).

(20) T. S. Lee, R. A. Krupa, F. Zhang, M. Hajimorad, W. J. Holtz, N. Prasad, S. K. Lee, and J. D. Keasling, *J. Biol. Eng.*, **5**, 12 (2011).

(21) T. K. Kim, J. J. Yoon, D. S. Lee, and T. G. Park, *Biomaterials*, **27**, 152 (2006).

(22) G. A. Van Aken, *Colloids Surf. A*, **190**, 333 (2001).

(23) X. Shi, L. Sun, J. Jiang, X. Zhang, W. Ding, and Z. Gan, *Macromol. Biosci.*, **9**, 1211 (2009).

(24) J. M. Gao, L. Niklason, and R. Langer, *J. Biomed. Mater. Res.*, **42**, 417 (1998).

(25) Y.-Y. Yang, T.-S. Chung, and N. P. Ng, *Biomaterials*, **22**, 231 (2001).

(26) H. Jeffery, S. S. Davis, and D. T. O'hagan, *Pharm. Res.*, **10**, 362 (1993).

(27) Q. Wang, S. Jamal, M. S. Detamore, and C. Berkland, *Mater. Res. Part A*, **96**, 520 (2011).

(28) Z. X. Meng, W. Zheng, L. Li, and Y. F. Zheng, *Mater. Chem. Phys.*, **125**, 606 (2011).

(29) L. Wang, L. Zheng, C. Y. Li, S. J. Dong, A. Lan, and Y. M. Zhou, *Biomed. Eng. Online*, **12**, 99 (2013).

(30) X. D. Yuan, B. A. Shah, N. K. Kotadia, J. Li, H. Gu, and Z. Q. Wu, *Pharm. Res.*, **27**, 1285 (2010).

(31) K. Zhao, Y. Zhang, X. Y. Zhang, C. Shi, X. Wang, X. H. Wang, J. Zheng, and S. J. Cui, *Int. J. Nanomedicine*, **9**, 4609 (2014).